PCCP

Accepted Manuscript

This article can be cited before page numbers have been issued, to do this please use: M. Prasad, F. Strubbe, F. Beunis and K. Neyts, *Phys. Chem. Chem. Phys.*, 2016, DOI: 10.1039/C6CP03544B.

View Article Online
DOI: 10.1039/C6CP03544B

Space Charge Limited Release of Charged Inverse Micelles in Non-Polar Liquids

Manoj Prasad*, Filip Strubbe, Filip Beunis and Kristiaan Neyts

LCP Group, ELIS Department, Ghent University, Technologiepark Zwijnaarde 15, 9052 Gent, Belgium

and

Center for Nano and Biophotonics, Ghent University, Technologiepark Zwijnaarde 15, 9052 Gent, Belgium

Abstract

Charged inverse micelles (CIMs) generated during a continuous polarizing voltage between electrodes in the model system of polyisobutylene succinimide in dodecane do not populate a diffuse double layer like CIMs present in equilibrium (regular CIMs), but instead end up in interface layers. When the applied voltage is reversed abruptly after a continuous polarizing voltage step, two peaks are observed in the transient current. The first peak is due to the release of regular CIMs from the diffuse double layers formed during the polarizing voltage step, which is understood on the basis of the Poisson-Nernst-Planck equations. The second peak is due to the release of a small fraction of generated negative CIMs from the interface layer. A model based on space charge limited release of the generated negative CIMs from the interface layer is presented and the results of the model are compared with several types of measurements. For the situation in which the bulk is deprived of regular CIMs and neutral inverse micelles, the results of the model are in agreement with the experimental results. However, for the situation in which regular CIMs and neutral inverse micelles are present, the

View Article Online
DOI: 10.1039/C6CP03544B

model shows discrepancies with the experiment for high voltages and high charge contents. These discrepancies are attributed to electrohydrodynamic flow caused by local variations in the electric field at the vicinity of the electrodes, which occur during the reversal voltage. Also the long term decrease of the amount of released generated CIMs is studied and it is found that the presence of regular CIMs and neutral inverse micelles speeds up the decrease. This study provides a deeper insight in the electrodynamics of CIMs and is relevant for various applications in non-polar liquids.

1. Introduction

Non-polar liquids have a low dielectric constant and the concentration of free charges is typically very low. The addition of surfactant molecules that contain polar groups can stabilize free charges and charged particles, in particular when the critical micelle concentration (CMC) is reached and inverse micelles can be formed[1]. In thermal equilibrium a small fraction of these inverse micelles is charged (to $+e$ or $-e$) and called charged inverse micelles (CIMs)[2–4]. The formation of CIMs, their charge stabilization and electrodynamical properties have been studied widely[2,3,5–11]. However, not all aspects of the charging dynamics have been clarified. Non-polar liquids with surfactants are used in inkjet printing[1], liquid toners[12], electrophoretic image displays[13–15] and many others applications[16–19].

To study the motion of CIMs in a non-polar medium, transient current measurements after the application of a voltage step over the electrodes of a planar cell have been used [10,11,20–23]. In this study, transient current measurements in response to a polarizing voltage step ($0 \rightarrow V_0$) and a reverse voltage step ($V_0 \rightarrow -V_1$) have provided insight about the generation mechanism and the dynamics of CIMs and the adsorption/desorption of CIMs at interfaces[20,24,25]. On the basis of transient electrical behavior, surfactant systems can be

View Article Online
DOI: 10.1039/C6CP03544B

categorized in two broad categories. The first category corresponds to the surfactant systems in which the generation rate of CIMs is so low that the bulk is almost depleted of CIMs when a polarizing voltage larger than 1 V is applied[23,25]. Surfactant systems such as polyisobutylene succinimide (PIBS), commonly known as OLOA 11K, Solsperse 13940, and sorbitan monooleate or Span 80 are in this category. The radius (r) of CIMs of these surfactants is larger than 3 nm. The surfactants OLOA 11K ($r \approx 5.5$ nm[11,25,26]) and Span 80 ($r \approx 4$ nm[26]) are non-ionic while Solsperse 13940 ($r \approx 8$ nm[26]) is an ionic surfactant. The second category includes surfactant systems such as ionic sodium dioctylsulfosuccinate or Aerosol OT (AOT) ($r \approx 1.6$ nm[2,3,26]) and non-ionic sorbitan trioleate or Span 85 ($r \approx 3$ nm[26,27]), in which the generation rate of CIMs is much higher than their transportation rate to the opposite polarity electrode on application of an electric field. Therefore, in these surfactant systems, the concentration of CIMs in the bulk always remains approximately equal to the equilibrium concentration[24,26]. Also, the behavior at interfaces of each category of CIMs is different, the CIMs of the first category surfactant systems end up in a diffuse double layer[28] while that of the second category CIMs form interface layers[24] at the electrodes. The difference in the interfacial electric behavior of CIMs leads to different transient currents. Detailed theoretical and experimental studies have been carried out for the first category of surfactant systems and various electrodynamical regimes, depending on the applied voltage and the charge content, have been identified[11,20,23]. Similarly, for the second category of surfactant systems exponentially decreasing currents are observed, which can be modeled as a resistor in series with interface capacitances[24].

For the first category of surfactant systems such as OLOA 11K and Solsperse, when the voltage is reversed abruptly after a continuous polarizing voltage step ($V_0 > 1$ V), two peaks are observed in the currents[23,25] while no peak is observed for the second category of surfactant system such as AOT. The occurrence of the first peak is understood well on the

View Article Online
DOI: 10.1039/C6CP03544B

basis of the Poisson-Nernst-Planck equations. It is observed that the integral of the first peak always remains the same because it is related to the fixed amount of CIMs present in equilibrium[23]. However, the integral of the second peak increases with increasing duration of the polarizing voltage step and eventually reaches a saturation level for high voltages. From this observation, it has been concluded that the second peak is a result of new charges generated during the quasi steady state of the polarizing voltage step[29].

Previously, we have reported on two studies about the properties of generated CIMs and the mechanism of their release[25,29]. In the first study, we showed that the mobility and the size of the generated CIMs are the same as that of the regular CIMs[25]. The other study investigated space-charge limited release of generated CIMs and pointed out that the newly generated CIMs do not populate the diffuse double layer at the electrodes like the regular CIMs, but instead end up in interface layers[29]. When the applied voltage is reversed or switched off only a small fraction of the negatively charged generated CIMs is released from the interface layer, these CIMs are termed as special CIMs or SCIMs. The release of SCIMs from the interface layer during the reversal or relaxation voltage results in a second peak in the current.

In this article, we examine the origin of the second peak by varying the duration and magnitude of the polarizing voltage step, the bulk thickness and the mass fraction of the surfactant. We propose a theoretical model for the release of generated negative CIMs from the interface layers and compare the results of the model with measurements performed in various situations. Finally, we study the long term decrease of the excess of generated CIMs with and without the presence of regular CIMs.

View Article Online
DOI: 10.1039/C6CP03544B

2. Materials and Methods

For the transient current measurements, test devices are used that consist of two parallel glass substrates coated with indium tin oxide (ITO) electrodes with overlapping area S = 1 cm^2. Quartz spherical balls mixed with ultraviolet curing glue (Norland) are used to hold the ITO coated glass substrates at a distance d from each other, with d = 7.6, 20 or 46 μm. The thicknesses are confirmed using the optical transmission spectrum. Solutions are prepared with mass fraction ϕ_m = 0.001, 0.003, 0.006, 0.012 and 0.024 of polyisobutylene succinimide (PIBS), commonly sold as OLOA 11K (Chevron Oronite) in dodecane (Aldrich, ε_r = 2). No particular measures were taken to eliminate traces of water or to purify the mixtures. The volume between the electrodes is filled with the prepared mixtures. Currents are measured using a custom built setup based on a Keithley 428 current amplifier. Before starting a measurement, equilibrium conditions are ensured in the device by short-circuiting the electrodes for 10000 s. Then, five types of experiments are performed that all provide some insight in the behavior of generated CIMs (see Fig.1).

The different types of experiments are illustrated in Fig. 1. In the first experiment (Type A) the effect of the polarizing voltage step duration on the reverse current is studied by increasing the duration t_0 (10 s to 10000 s) of the polarizing voltage step $0 \rightarrow V_0$ (V_0 >1 V) while keeping a constant duration of the reverse (t_1 = 200 s) and relaxation voltage steps (t_{s0} = 10000 s). In the second type of experiment (Type B) the effect of the voltage V_2 on the current due to the release of the generated CIMs is studied after the removal of regular and neutral inverse micelles (IMs). The experimental sequence is: polarizing voltage step $0 \rightarrow V_0$ (V_0 = 5V) with duration t_0 =10000 s; short-circuiting for t_{s1} = 100 s. Then using a suction pump the liquid between the substrates is sucked out and the space between the substrates is replaced by air. Afterwards, the space between the substrates is refilled with pure dodecane and the same suction process is repeated. This suction and filling process is repeated 10 times to ensure that

View Article Online
DOI: 10.1039/C6CP03544B

the liquid in the volume is completely replaced with pure dodecane[29]. Afterwards, the electrodes are re-connected to the measurement setup, a voltage step $0 \rightarrow V_2$ is applied for t_2 = 200 s and the device is short circuited for a time t_{s2}. In the third type of experiment (Type C) the effect of the reverse voltage step on the reverse current is studied by increasing the magnitude of the reverse voltage step ($V_0 \rightarrow -V_1$) while keeping constant durations for the polarizing (t_0 = 10000 s), reverse (t_1 = 200 s) and relaxation voltage steps (t_{s0} = 10000 s). In the fourth type of experiment (Type D) the decrease in the number of the generated CIMs is studied as a function the short circuit duration t_{s3}. The experimental sequence is: polarizing voltage step (V_0 = 5 V) of duration t_0 = 10000 s; short circuiting for a duration t_{s3} between 20 s and 5000 s; voltage step $0 \rightarrow V_3$ (V_3 = 5 V) for t_3 = 20 s and short circuiting for t_{s0} = 10000 s. In the fifth type of experiment (Type E) the decrease in the number of the generated CIMs is studied with increasing the short circuit duration t_{s4} in the absence of regular CIMs and neutral IMs. The experimental sequence (Type E) is identical to that of experiment type B until the filling with pure dodecane. Afterwards, a voltage step $0 \rightarrow V_4$ (V_4 = 5 V) is applied across the electrodes for a duration of t_4 = 20 s and then the electrodes are short circuited for t_{s4} (t_{s4} = 1000 to 50000 s). Then, again a voltage step $0 \rightarrow V_4$ is applied. By measuring the initial current after applying the polarizing voltage pulse V_0 and the integral of the current pulse over t_0 (without the quasi-steady state current) as described elsewhere[23], the mobility of the CIMs has been determined as 1320 $\mu m^2/Vs$.

View Article Online
DOI: 10.1039/C6CP03544B

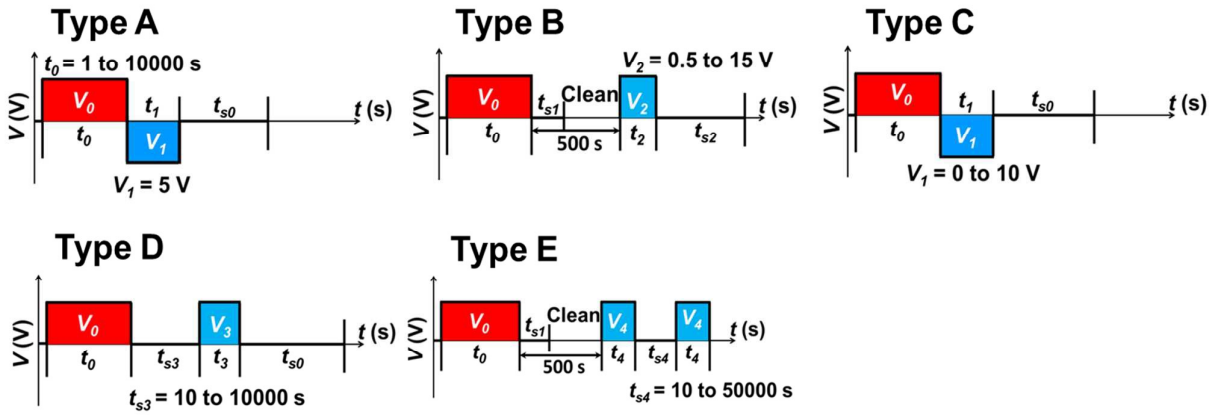

Figure 1: Schematic illustration of the voltage sequences for various types of transient current experiments. Type A: the duration t_0 is varied. Type B: the bulk liquid is replaced by dodecane (clean) and V_2 is varied. Type C: V_1 is varied. Type D: t_{s3} is varied. Type E, t_{s4} is varied.

3. Theoretical Model

In this section a one-dimensional numerical simulation model is introduced that describes the transport of CIMs and the release of SCIMs from the interface layer. We consider the case when the space between two parallel electrodes, separated at a distance d, is filled with a mixture of nonpolar liquid and surfactant. In thermal equilibrium and in the absence of an electric field, a small fraction of inverse micelles is charged due to a disproportionation mechanism[10,25] leading to an equilibrium concentration of positively and negatively charged inverse micelles: $\bar{n} = n_+ = n_- = \sqrt{K_{eq}}\,\bar{n}_o$. Here, $\bar{n}$ and $\bar{n}_o$ are the initial concentrations of charged and uncharged inverse micelles respectively and K_{eq} is the equilibrium constant. The CIMs present in the equilibrium are referred to as regular CIMs. When there is a field and a concentration gradient, drift and diffusion of the regular CIMs result in a flux of positive or negative CIMs: $\Psi_\pm = \pm n_\pm \mu E - D\frac{\partial n_\pm}{\partial x}$. Here x is the position between the electrodes which are situated at $x = 0$ and $x = d$, μ is the mobility of the CIMs, E is the electric field and D is the

View Article Online
DOI: 10.1039/C6CP03544B

diffusion constant of the CIMs. The diffusion constant and the mobility are linked by Einstein's relation: $D = \mu k_B T/e$.

The observed quasi steady-state currents are well explained by the bulk disproportionation mechanism, in which two neutral inverse micelles collide and exchange a charge, resulting in a positive and a negative CIM[2,10,8]. In contrast to the dissociation of single neutral micelles, the disproportionation mechanism can explain the quadratic dependency of the quasi steady-state current on the surfactant concentration (which is also proportional to the neutral inverse micelle concentration)[10,25]. In the present model we assume that there are three types of CIMs that can be generated in the bulk in the presence of an electric field as the result of disproportionation. For each reaction on average the following CIMs are created: 1 positive (n_{s+}) and 0.95 negative (n_{s-}) CIMs that will stick to the interface layer and are never released again, and 0.05 special negative CIMs (n_{SCIMs}) or SCIMs that can be released from the interface layer[29]. The mobility and diffusion constant of these CIMs are the same as that of the regular CIMs[25]. For each of them we can define a flux Ψ_{s+}; Ψ_{s-}; Ψ_{sCIM}, which satisfy similar relations as $\Psi_{\pm}$. The low generation rate constant β[10] (order 10^{-24} m^3/s) for OLOA 11K in dodecane leads to the conclusion that the concentration of the neutral inverse micelles n_o remains approximately equal to the original value $\bar{n}_o$.

Ignoring the electric field dependency of β, ignoring recombination of CIMs and taking into account the above-mentioned proportions 100%, 95% and 5% in which the various CIMs are generated in the presence of an electric field, the continuity equations for the different types of CIMs can be written as:

$$\frac{\partial n_{\pm}}{\partial t} = -\frac{\partial}{\partial x}(\Psi_{\pm}) \quad (1)$$

$$\frac{\partial n_{s+}}{\partial t} = -\frac{\partial}{\partial x}(\Psi_{+}) + \beta n_0^2 \quad (2)$$

View Article Online
DOI: 10.1039/C6CP03544B

$$\frac{\partial n_{s-}}{\partial t} = -\frac{\partial}{\partial x}(\Psi_{s-}) + 0.95\beta n_0^2 \quad (3)$$

$$\frac{\partial n_{SCIMs}}{\partial t} = -\frac{\partial}{\partial x}(\Psi_{SCIMs}) + 0.05\beta n_0^2 \quad (4)$$

The electric field between the electrodes is governed by Gauss's equation:

$$\varepsilon_o \varepsilon_r \frac{\partial E}{\partial x} = \rho \quad (5)$$

In this equation, $\rho = e(n_+ - n_- + n_{s+} - n_{s-} - n_{SCIMs})$ is the charge density. By integrating equation 5 we find $E(x) = E(0) + \int_0^x \frac{\rho}{\varepsilon_o \varepsilon_r} dx$ and by using $E(0) = \frac{V}{d} - \frac{1}{d}\int_0^d \int_0^x \frac{\rho(x\prime)}{\varepsilon_o \varepsilon_r} dx' dx$, we can find the electric field:

$$E(x) = \frac{V}{d} + \frac{1}{\varepsilon_o \varepsilon_r d}\left(\int_0^x \rho(x')x'dx' + \int_d^x \rho(x')(d - x')dx'\right) \quad (6)$$

The current in the external circuit is given by[11,25]:

$$I(t) = (eS/d)\int_0^d (\Psi_+ - \Psi_- + \Psi_{s+} - \Psi_{s-} - \Psi_{SCIMs})\, dx \quad (7)$$

Initially, at t = 0, when the device is in equilibrium, the regular CIMs are uniformly distributed and we assume that the concentration of generated CIMs is zero. Thus, the initial conditions at t = 0 are given by:

$$n_+ = n_- = \bar{n} \quad (8)$$

$$n_{s+} = n_{s-} = n_{SCIMs} = 0 \quad (9)$$

Now we discuss the boundary conditions. Regular CIMs form a double layer in the bulk, while the different types of generated CIMs ($n_{s\pm}$ and n_{SCIMs}) are adsorbed at the surface and form the interface layers with thickness Δ. Previous studies show that the distance between the charges in the interface layer and the electrode (α.Δ with α<1) is so small, that the charges do not affect the electric field in the bulk significantly[23], and therefore Δ has to be much smaller than 1 nm.

View Article Online
DOI: 10.1039/C6CP03544B

For the regular CIMs there is no flux into the interface layers and blocking boundaries conditions are used:

$$\Psi_{\pm}\,(x = \Delta) = \Psi_{\pm}\,(x = d - \Delta) = 0 \qquad (10)$$

When they reach the interface layers the generated CIMs get adsorbed with their charge situated at $x = \Delta$ and $x = d - \Delta$. Therefore their bulk concentration can be set equal to zero at the corresponding locations:

$$n_{s\pm}(x = \Delta) = n_{s\pm}(x = d - \Delta) = 0 \qquad (11)$$

For the negative SCIMs we consider two cases. First we consider the case when the electric field in the bulk near the interface layer is pointing away from the interface. In this case the SCIMs are adsorbed in the interface layer, just like the other generated CIMs

$$n_{SCIMs}\,(x = \Delta) = 0, \quad \text{when } E(x = \Delta) > 0 \qquad (12)$$

$$n_{SCIMs}(x = d - \Delta) = 0, \text{ when } E(x = \Delta) < 0 \qquad (13)$$

The flux of SCIMs going into and out of the interface layer is linked to the surface densities of SCIMs in the interface layer N_{SCIMsL} situated at $x = \Delta$ and N_{SCIMsR} situated at $x = d - \Delta$ by the continuity equations:

$$\frac{\partial N_{SCIMsL}}{\partial t} = -\Psi_{SCIMs}\,(x = \Delta) \qquad (14)$$

$$\frac{\partial N_{SCIMsR}}{\partial t} = \Psi_{SCIMs}\,(x = d - \Delta) \qquad (15)$$

When the field in the bulk near the positive electrode becomes less than zero, SCIMs can be released from the interface layer. We assume here that the release of negative SCIMs is governed by field clamping, which means that as many charges are released as needed to keep the field at $x = \Delta$ (or at $x = d - \Delta$) equal to zero[30,31]. This continues until all the negative charges are released. At that moment the field in the bulk near the interface layer can start to point into the electrode.

View Article Online
DOI: 10.1039/C6CP03544B

During field clamping we have $E(x = \Delta) = 0$ and in the electrode $E(x = d - \Delta) = 0$ which means that the charge in the interface layer remains exactly opposite to the charge on the electrode. By taking the time derivative of both quantities we can find the flux of SCIMs:

$$\Psi_{SCIMs}(x = \Delta) = -\frac{I(t)}{eS}, \text{ as long as } N_{SCIMsL} > 0 \quad (16)$$

The decrease of N_{SCIMsL} is found by the continuity equation given earlier. When its value becomes zero, no more SCIMs can be released:

$$\Psi_{SCIMs}(x = \Delta) = 0, \text{ when } N_{SCIMsL} = 0 \quad (17)$$

With similar formulas applying for the release of SCIMs near the $x = d$ interface.

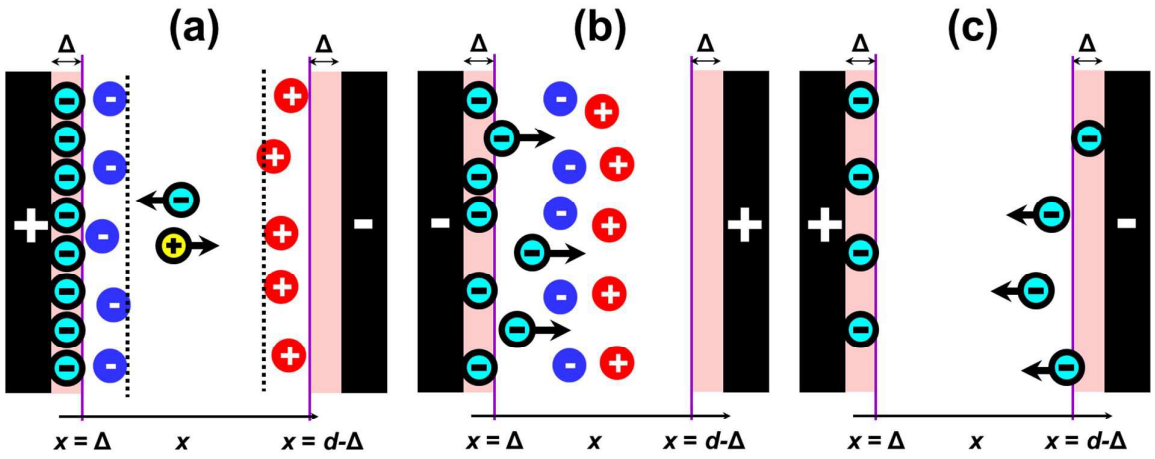

Figure 2: Representation of the device with two parallel electrodes at distance d with area $S = 1$ cm^2. The device is filled with a suspension of OLOA 11K in dodecane. The regular CIMs are shown in red and blue while the generated CIMs are in cyan and yellow. (a) Shows the response to a polarizing voltage step ($0 \rightarrow V_0$) with the formation of diffuse double layers and interface layers (light pink color). The SCIMs in the interface layer are shown in cyan, the other adsorbed CIMs are not shown. (b) Shows the release of regular CIMs and SCIMs (cyan) when the voltage is reversed ($V_0 \rightarrow -V_1$). (c) Shows interface layers with SCIMs after cleaning the device and the release when a voltage is applied.

The set of equations for the CIMs fluxes are numerically solved. This involves solving the differential equations 1-5, using the initial conditions of equations 8-9 and the boundary

View Article Online
DOI: 10.1039/C6CP03544B

conditions of equations 10-17. The electric currents in the external circuit are calculated using equation 7.

4. Experimental Results and Simulations

In this section we provide the results for the transient current measurements that are described in section 3. Typically series of measurements are carried out to investigate the influence of the short circuit time or the amplitude of the voltage pulse.

4.1. Reverse Current for Different Pulse Durations

In this subsection we describe the results for the experiment of type A: reversal transient current as a function of the duration of the polarizing voltage step, the cell thickness and mass fraction (ϕ_m) of OLOA 11K. Fig. 3 (a) shows that, for a short duration of the polarizing voltage step (t_0 =10 s), there is a single peak in the reverse current, which is well-understood on the basis of the Poisson-Nernst-Planck equations[23]. For longer durations of the polarizing voltage step (t_0 > 100 s) there is a second peak in the current, starting at t_1 = 0.15 s, which grows with the duration of the polarizing voltage step t_0, and saturates for t_0 > 3000 s. The effect of the cell thickness and the duration of the polarizing voltage is evaluated by integrating the current of the second peak over the interval t_1 = [0.15 s, 1 s] to obtain Q_{sp}. Fig. 3 (b) indicates that the saturation level of Q_{sp} scales roughly linearly with the cell thickness (for d >10 μm) as $\left(8.8 \times 10^{-4}\,\frac{\mathrm{C}}{m}\right) \times d(\mathrm{m})$. Fig. 3 (c) shows that an increase in the mass fraction ϕ_m of the surfactant leads to an increase in Q_{sp}. The saturation level of Q_{sp} (for long t_0) is approximately proportional to ϕ_m (for $\phi_m \leq 0.012$).

View Article Online
DOI: 10.1039/C6CP03544B

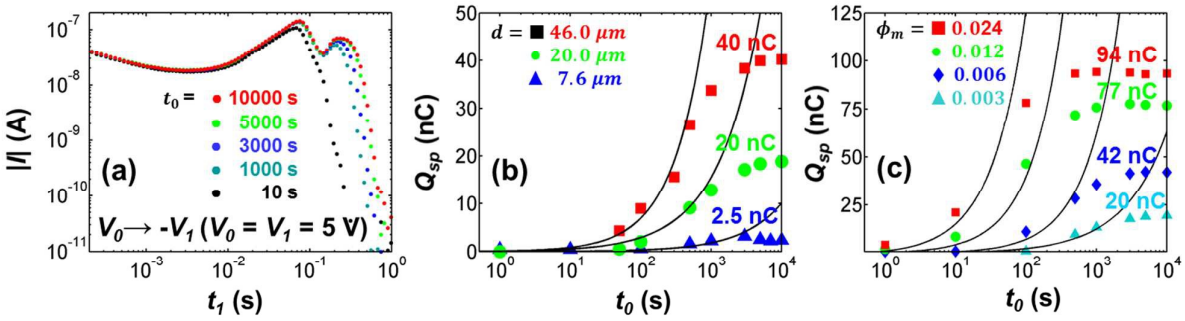

Figure 3: Reverse transient current experiment of type A for OLOA 11K in dodecane. (a) Reverse transient current for different durations t_0 of the polarization pulse for a device with d = 20 μm and ϕ_m = 0.003. (b) Integral of the second peak Q_{sp} on a semilogarithmic scale as a function of the duration of the polarizing voltage pulse, for different cell thicknesses d, with ϕ_m = 0.003. (c) Integral of the second peak Q_{sp} on a semilogarithmic scale as a function of the duration of the polarizing voltage pulse for different mass fraction ϕ_m for a device with d = 20 μm. The black lines show approximately linear fit with the experimental data.

The charge generated during a polarizing voltage step (V_0 > 1 V) scales as[10,25] $Q_g = \beta n_o^2 edSt_0$. Fig. 3(b) shows that the integral of the second peak Q_{sp} is also roughly linear with the duration of the polarizing voltage step t_0 (shown by black line in Fig. 3 (a) & (b)) and the saturated integral of the second peak scales with the cell thickness d (for d >10 μm) as $\left(8.8 \times 10^{-4} \frac{\mathrm{C}}{m}\right) \times d(\mathrm{m})$, which indicates that the second current peak is related to the generation of new charges in the bulk. Fig. 3(c) shows that the saturation level Q_{sp} scales linearly with ϕ_m according to 6540 nC× ϕ_m, for $\phi_m \leq 0.012$ (and not quadratically as Q_g, as will be discussed later). Therefore, the saturation level of the integral of the second peak scales proportionally with the cell thickness and with ϕ_m (for $\phi_m \leq 0.012$) as $\left(0.34 \frac{\mathrm{C}}{m}\right) \times \phi_m d(m)$. For the concentration ϕ_m= 0.003, the maximum integral of the second peak Q_{sp} = 20 nC is approximately 6.7 % of the charge Q_g = 300 nC generated during a polarizing voltage step of 10000 s.

View Article Online
DOI: 10.1039/C6CP03544B

4.2. Reverse Current for Cleaned Device

Fig. 4 shows experiments of type B in which, after a polarizing voltage step, the bulk is replaced with pure dodecane and a positive voltage pulse is applied. The experiments are carried out for two concentrations: (a) ϕ_m = 0.003 and (b) ϕ_m = 0.006, yielding for the integral of the measured currents Q^* during t_2 respectively 8 nC and 16 nC. The experiment of type B has been repeated for a negative voltage pulse $0 \rightarrow -V_2$. In this case the shape of the transient current and the integral values are about identical to those shown in Fig. 4. This indicates that the SCIMs are redistributed equally on both the electrodes during the short circuit time[29] $t_{s1,}$ as depicted in Fig. 2 (c). The total amount of charge is then the double of what is measured for a voltage step, namely 16 nC for $\phi_m = 0.003$ (Fig. 4 (a)) and 32 nC for ϕ_m = 0.006 (Fig. 4 (b)), which is approximately matching with the saturated integral of the second peak shown in Fig. 3 (c).

The simulation of the transient current is based on the release of SCIMs from the interface layer near the $x = d$ electrode, when the field at $x = d - \Delta$ remains clamped to zero as explained in section 3. The good agreement between the measurements and the simulations confirms that the SCIMs are indeed released at zero field. We can recognize two particular regions in the time dependency of the simulated currents in Fig. 4: up to about 10^{-3} s the current decreases and is proportional to $t^{-1/2}$; and between about 10^{-1} s and 10 s the current remains approximately constant. We will now explain these two particular regimes, based on the model that has been described in section 3.

After cleaning and removing all the regular CIMs from the bulk, a charge corresponding to $-Q^*$ remains in both interface layers and the field in the bulk is zero. When the voltage pulse V_2 is applied to the electrode at $x = 0$, a charge $-Q = -CV_2$ is supplied to the electrode at $x = d$, with $C = (\varepsilon_0 \varepsilon_r S)/d$ the capacitance of the device. To maintain the field at $x = d - \Delta$ equal to

View Article Online
DOI: 10.1039/C6CP03544B

zero an equal charge $-CV_2$ is released from the interface layer at $t = 0$. At short time scales, drift in the field can be neglected compared to diffusion, and the motion of the SCIMs is determined by free diffusion from the surface. This means that the average distance from the electrode increases with time as $\sqrt{2Dt}$. This leads to the diffusion current:

$$I_s(t) = \frac{CV_2}{d}\frac{\partial}{\partial t}(\sqrt{2Dt}) = \frac{\varepsilon_o \varepsilon_r S V_2}{d^2}\sqrt{\frac{\mu k_B T}{2et}} \quad (18)$$

In the double logarithmic graph of Fig. 4 this equation is represented by a straight line. It matches numerical simulations for small values of t_2.

Now we will develop a model for the time interval where the current remains practically constant. Let us assume that the current density J which is due to SCIMs is independent of the position[31] and that we can neglect diffusion. The current density is then given by:

$$J = n_{SCIM}(x) e \mu E(x) \quad (19)$$

Combining this equation 19 with Gauss's equation and replacing ρ by $-en_{SCIMs}$, gives:

$$\varepsilon_0 \varepsilon_r \frac{\partial E(x)}{\partial x} = -\frac{J}{\mu E(x)} \quad (20)$$

After separating the variables x and E and integrating the above equation from x to $d - \Delta$ using the boundary condition $E(d - \Delta) = 0$, one obtains:

$$J = \frac{\mu \varepsilon_o \varepsilon_r E(x)^2}{2(d-\Delta-x)} \quad (21)$$

Equation 21 can be written as:

$$E(x) = \sqrt{\frac{2J(d-\Delta-x)}{\mu \varepsilon_o \varepsilon_r}} \quad (22)$$

Integrating equation 22 over the thickness and neglecting Δ yields:

$$V_2 = \int_0^d \sqrt{\frac{2J(d-x)}{\mu \varepsilon_o \varepsilon_r}}\, dx = \sqrt{\frac{8d^3 J}{9\varepsilon_o \varepsilon_r \mu}} \quad (23)$$

View Article Online
DOI: 10.1039/C6CP03544B

The current J is also equal to the steady state current measured in the external circuit. Then, using $J = I_{ss}/S$ equation 23 yields the well-known Mott-Gurney formula which is used to calculate the value of currents in the stationary state of space charge limited release of charges[30,31].

$$I_{ss} = \frac{9\varepsilon_o\varepsilon_r\mu S{V_2}^2}{8d^3} \qquad (24)$$

Fig. 4 shows that the Mott-Gurney formula indeed represents the observed (and simulated) current well. The time at which the stationary state current comes to an end can be estimated from the total charge that is present in the interface layer and the steady state current: $t_{ss} = Q^*/I_{ss}$.

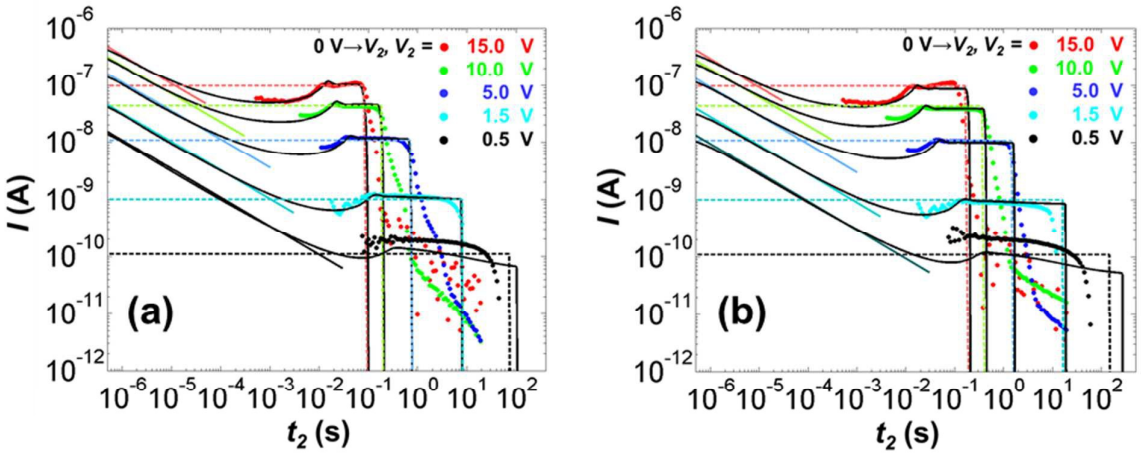

Figure 4: Measured transient currents (colored dots) for the experiment type B (after cleaning) are compared with the simulated currents (black lines) for a device with d = 20 µm which was filled with a suspension (a) ϕ_m = 0.003 (b) ϕ_m = 0.006 of OLOA 11K in dodecane. The colored lines show the calculated currents using equation (18) while the dotted color lines correspond to the Mott-Gurney equation.

The time variation of the electric field distribution and the charge distribution is shown in Fig. 5 for a number of times, when a voltage pulse of 5 V is applied for the case of ϕ_m = 0.003. Up to about 10 ms, free diffusion of SCIMs is observed from the interface at $x = d$. Between t

View Article Online
DOI: 10.1039/C6CP03544B

= 45 ms and t = 185 ms the field is approximately proportional to the square root of the position x, which corresponds to the Mott-Gurney regime of space charge limited current.

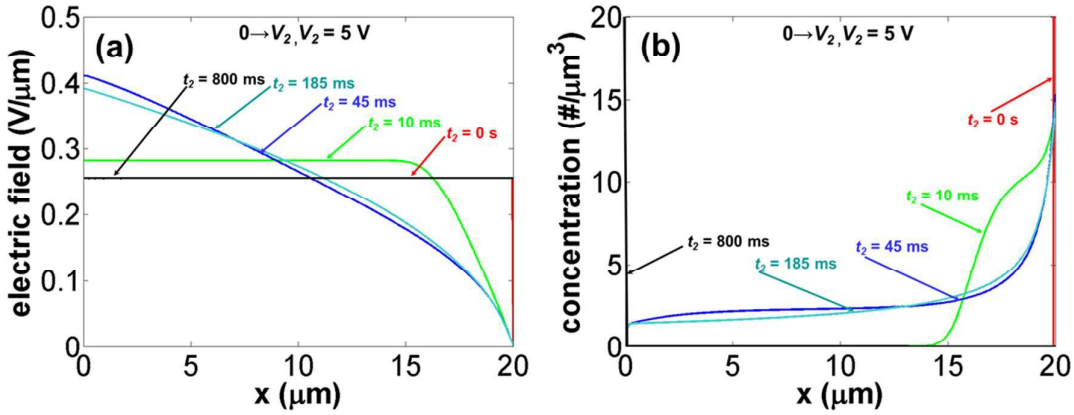

Figure 5: Simulated transient profile of (a) the electric field (b) the concentration of the released SCIMs for the experiment type B in a device with d = 20 μm with ϕ_m = 0.003. The SCIMs are released from the interface layer situated at the right electrode (shown by a red line) clamping the field to zero. The stationary state is reached around 45 ms and lasts up to 800 ms.

4.3. Reverse Current for Different Voltages

A comparison between the reverse transient current measurements and simulations for the experiment type C (variation of the applied voltage), for different concentrations of surfactant (ϕ_m = 0.001 or 0.003) and different thicknesses (d = 20 μm or d = 46 μm) is shown in Fig. 6. The initial transient current and the first peak are due to the motion of regular CIMs from the double layer, which was formed during the polarizing voltage step. The second peak or shoulder after the first peak, is due to the release of SCIMs from the interface layer when the field near x = 0 becomes zero. Since the shape and the origin of the first peak have been explained earlier in detail[23], in this article we focus on the second peak.

View Article Online
DOI: 10.1039/C6CP03544B

In Fig. 6 (a) the measurements are in excellent agreement with the simulation results (except for V_1 = 0 V), which indicates the validity of the assumptions. In Figs. 6 (b), (c) and (d), corresponding to higher concentrations and/or larger thicknesses, even though the first peak is described well by the simulations, there is a discrepancy since the measurements show a second peak while the simulations show only a shoulder after the first peak.

The integral of the current in the second peak (Q_{sp}) does not depend on the amplitude of the voltage V_1 and is given by Q_{sp} = 8, 23, 14 and 45 nC for the experiments in Figs. 6 (a), (b), (c) and (d) respectively. The integrals of the measured transient correspond well with the integrals of the simulated transient currents. This means that the same amount of charge is released but quicker (second peak) than predicted by the simulations for voltages larger than 1 V.

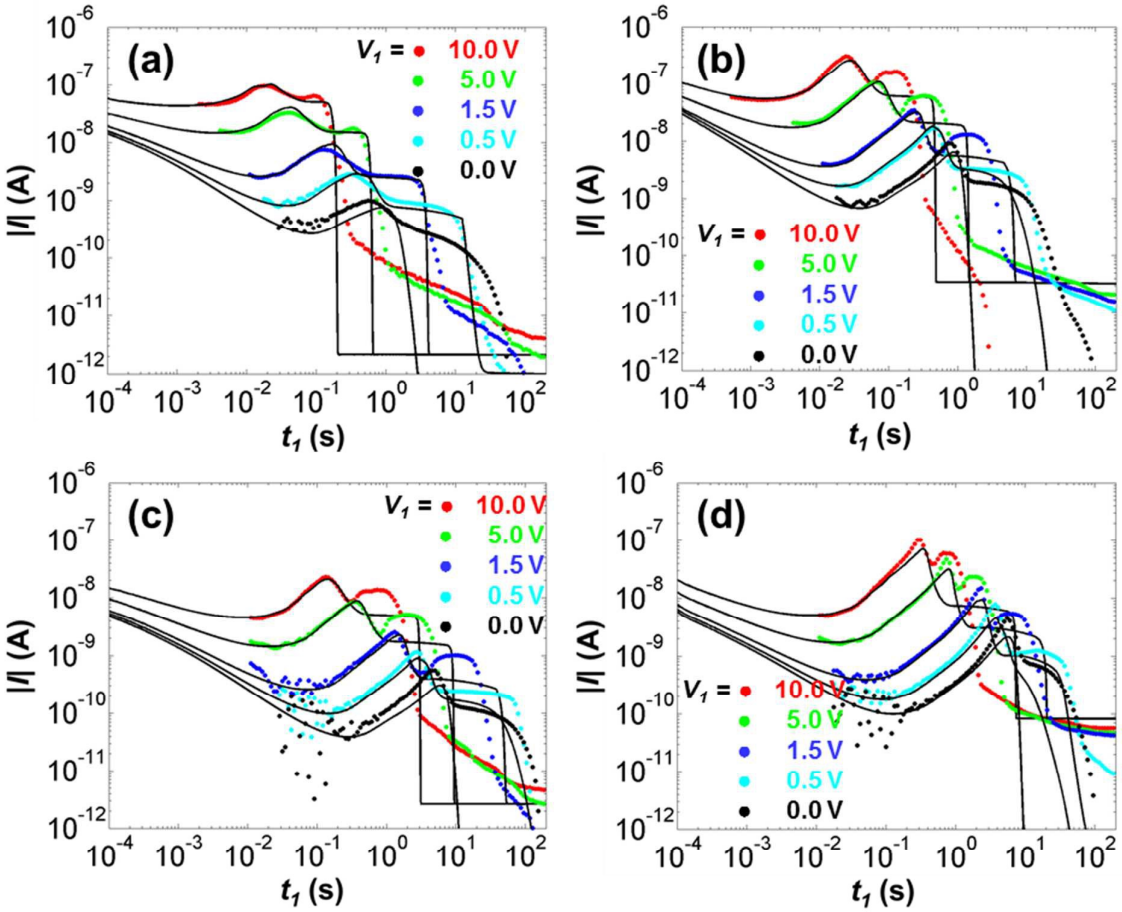

View Article Online
DOI: 10.1039/C6CP03544B

Figure 6: Measured transient currents ($|I|$) (colored dots) for the experiment type C are compared with the simulated currents (black lines) for 5 V→-V_1. The measurements are performed on devices with thickness d filled with a suspension of OLOA 11K in dodecane (a) d = 20 µm with ϕ_m = 0.001 (b) d = 20 µm with ϕ_m = 0.003 (c) d = 46 µm with ϕ_m = 0.001 (d) d = 46 µm with ϕ_m = 0.003.

Fig. 7 shows the simulated transient profile of the electric field and the concentration of negative charges for the experiment of type C (reverse current after a long polarization pulse) in a device with d = 20 µm filled with a suspension with ϕ_m = 0.001, which corresponds to the values of Fig. 6 (a). Immediately after reversing the polarity of the voltage (V_0→-V_1, V_0 = V_1 = 5 V), CIMs move away from the electrodes into the bulk since the field at x = Δ is positive (not shown). At t_1 = 21 ms the field E(Δ) decreases to zero, negative SCIMs are released from the interface layer at x = Δ and the field there remains clamped to zero up to 490 ms as shown in Fig. 7(a). Between t =110 ms and t = 490 ms the field distribution in Fig. 7 (a) remains more or less stationary. The relation with x is more or less a square root dependency (corresponding to the Mott-Gurney formula), except for a few µm near x = 0 because of the influence of the double layer. At t = 800 ms all the negative CIMs and SCIMs have arrived near the electrode at x = d.

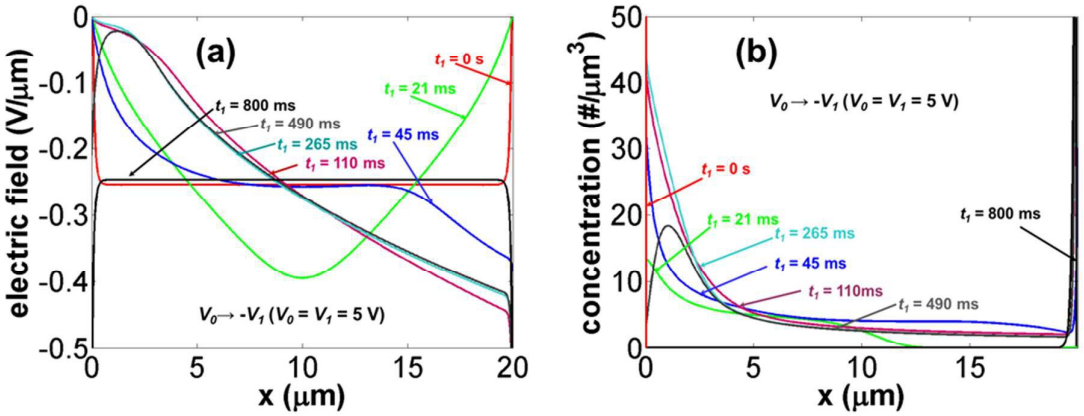

View Article Online
DOI: 10.1039/C6CP03544B

Figure 7: Simulated transient profile of (a) the electric field (b) the combined concentration of negative CIMs and SCIMs for the experiment of type C in a device with d = 20 μm filled with a suspension ϕ_m = 0.001 OLOA 11K in dodecane. The SCIMs are released from the interface layer near x = 0. As long as SCIMs are released from the interface layer at x = 0 the field there remains zero.

4.4. Long Term Decrease of the Number of SCIMs

In the following section we study the long term decrease of SCIMs which are generated during a polarizing voltage step ($0 \rightarrow V_0$, V_0 = 5 V) of duration t_0 = 10000 s. Two types of experiments were performed. In the first experiment (Type D), we investigate the influence of a long short circuit time t_{s3} on the transient current. Fig. 8(a) shows the transient currents for a device with d = 20 μm filled with ϕ_m=0.003 OLOA 11K in dodecane for five different short circuit times. It is clear that the current peak due to the release of SCIMs strongly decreases when the short circuit time is extended over several 1000 s. The current (until the peak) due to regular CIMs is unaffected by the short circuit time. To obtain a value for the decay time of the SCIMs in the interface layer, we have integrated the charge in the second peak Q_{sp} and plotted this value as a function of the short circuit time t_{s3} in Fig. 8(b) on a semilogarithmic scale. The decay is roughly exponential with an average decay time of 1000 s. The experiment has been repeated for ϕ_m= 0.001, 0.003 and ϕ_m=0.006 and the values of Q_{sp} have also been plotted in Fig. 8 (b). The decay times are 1700 s, 1000 s and 700 s respectively.

By using the cleaning procedure before applying the long short circuit time, we can investigate if the uncharged inverse micelles or CIMs in the bulk play a role in the decrease of the SCIMs in the interface layer. This means that the experiment of type E is carried out with variable duration of the short circuit time. The transient currents are shown in Fig. 8 (c). First of all we remark that the transient currents behave as in the case of field clamping: the current increases to a stationary value and then decreases abruptly to zero (as in Fig. 4). This indicates

View Article Online
DOI: 10.1039/C6CP03544B

that after cleaning and the long short circuit time there are SCIMs in the interface layer and no CIMs in the bulk of the layer. We can notice that the total charge of SCIMs that is released decreases with increasing short circuit time. The integral is shown in Fig. 8 (d). The average decay time is about 7000 s. The fact that this decay time is much longer than in Fig. 8 (c) indicates that either the CIMs or the neutral inverse micelles play a role in the decrease of the SCIMs in the interface layer.

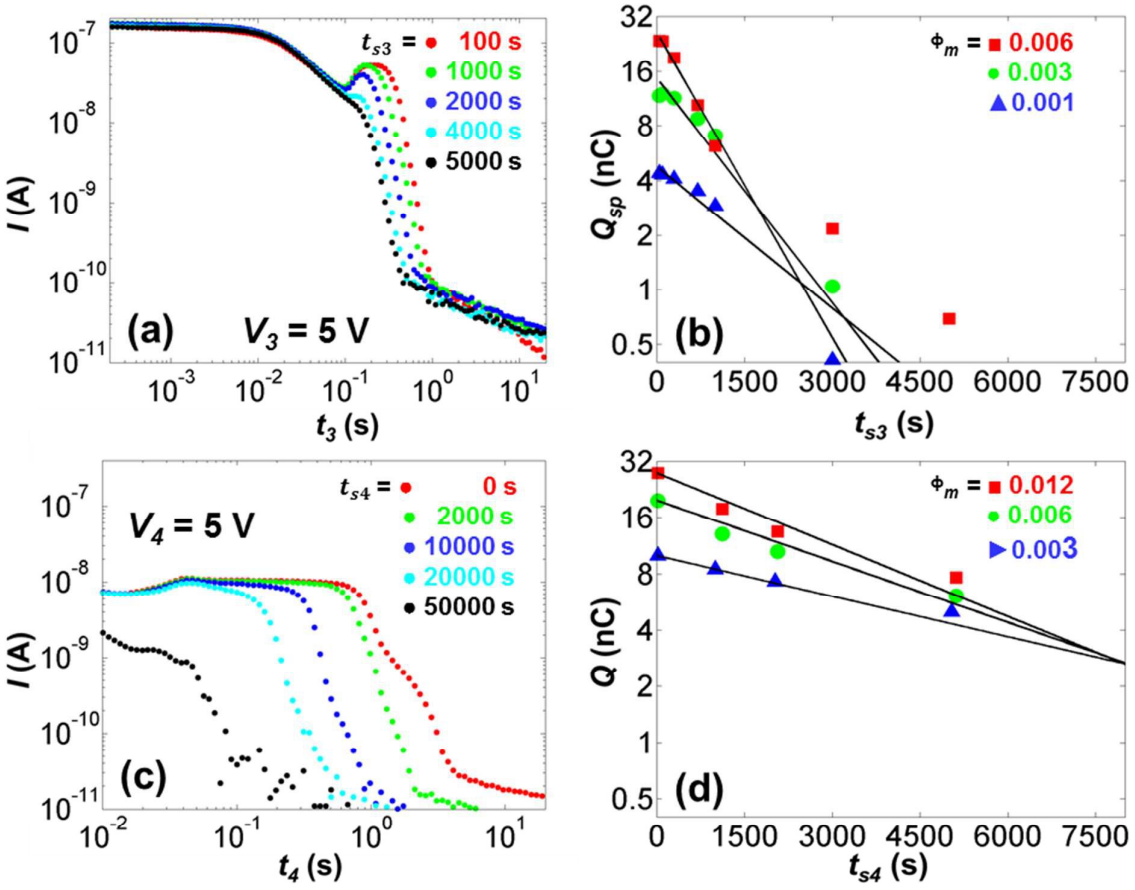

Figure 8: Results of the experiment types D (a & b) and E (c & d), which show the long term decrease of SCIMs, generated during a polarizing voltage step (0→V_0, V_0 = 5 V) of 10000 s in a device with d = 20 µm and filled with OLOA 11K (ϕ_m = wt. fraction) in dodecane. (a) Transient currents for different values of the short circuit duration t_{s3} for ϕ_m = 0.003 in experiment D. (b) Integral of the peak plotted on a semilogarithmic scale as a function of the short circuit duration t_{s3} and fitted with an exponential (lines). (c) Transient currents for different values of the short circuit duration t_{s4} for ϕ_m = 0.003 in experiment E (after cleaning the cell). (d)

View Article Online
DOI: 10.1039/C6CP03544B

Integral of the peak plotted on a semilogarithmic scale as a function of the short circuit duration t_{sd} and fitted with an exponential (lines).

5. Discussion

In this section we discuss a number of remarkable results that have been presented in section 4 and try to provide appropriate explanations. First we consider the saturation of the charge Q_{sp} as illustrated in Fig. 3(b) and (c) and the relation with the generated charge Q_g. We know that CIM that are generated during the polarizing pulse are separated and move to the electrode with the opposite polarity. They do not reside in the double layer (the first peak in Fig. 3(a) remains unchanged), but contribute to the interface layer. If we assume that the interface layer consists of a single layer of CIMs with radius[26] r = 5.5 nm, then we can estimate how much charge the interface layer in our device may contain. The formula for the maximum charge is $Q_{max}= f_c eS/(\pi r^2)$ with f_c = 0.91 the maximum packing density of circles in a 2D plane[32] which yields for our device Q_{max}=153 nC. For thick cells, high concentrations of OLOA 11K and long durations of the polarizing pulse, the generated charge exceeds this value by a large amount: $Q_{max}<<Q_g$, *e.g.* for $\phi_m = 0.012$, $Q_g \approx 30Q_{max}$. This indicates that not all the CIMs can be accommodated in the interface layer corresponding to a single layer of micelles. An explanation for this could be that these CIMs release their charge at the electrode and become uncharged. By electrical measurements we cannot discern if a charged ion remains at the surface or if there is a Faradaic current flowing into the electrode. The saturation of Q_{sp} may be linked to the decay rate of the SCIMs in the interface layer in the presence of uncharged (or charged) micelles. In Fig. 8 (b) we observed a decay rate of the order of 1000 s for SCIMs at the interface layer in the absence of an applied voltage. An equilibrium between generation and decay (also in the presence of a voltage) may explain the time at which saturation takes place.

View Article Online
DOI: 10.1039/C6CP03544B

What could be the reason that 5% of the negative CIMs (the so-called SCIMs) remain in the interface layer and can be released after the voltage is switched, while no positive generated micelles are released? We propose that the difference in the behavior can be explained by the location of the charge in the CIMs. We assume that in most of the generated CIMs (95% of the negative and all of the positive generated CIMs) the charge is located near the surface of the micelle surface. As a result the charge (or a small charged molecule) is transferred to the electrode surface. However, for 5% of the negatively charged generated CIMs the charge is not at the surface of the CIM and is not released when the SCIM reaches the interface layer. These micelles can be released after reversal of an appropriate electric field.

The discrepancies between the measurements and the simulations in the case of experiment type C (Fig. 6 b, c, and d) for higher concentrations or thicknesses can be explained by considering electrohydrodynamic (EHD) flow[23]. EHD flow has been observed by tracking tracer particles in response to a voltage step[23]during the reverse voltage pulse when the transport by positive and negative CIMs in a one-dimensional solution becomes unstable, and also transverse fluxes in the y and z direction occur. The result of the 3D EHD flow is that the released SCIMs are transported faster towards the opposite electrode, and the current in the second peak is larger and shorter (Fig. 6 (b, c and d)). With or without EHD the total transported charge remains the same, e.g. 23 nC for Fig. 6 (b). For the case of Fig. 6 (d), EHD flow occur during the release of regular CIMs which explains the mismatch between measurements and simulations during the first peak.

We will now discuss the discrepancy between measurements and the simulations for low voltages (experiment type C, Fig. 4 and 6) ($V_1 < 0.5$ V). In the simulation model the SCIMs are released when the field changes sign near the electrodes (in the interface layer) keeping the field equal to zero. The discrepancy with the experiments, namely that the shoulder is missing in the simulations, may be explained by the fact that the SCIMs can be released by

View Article Online
DOI: 10.1039/C6CP03544B

thermal energy, even when the electric field yields a (small) force towards the electrode surface. This is confirmed by the observation of currents for the experiment type C ($V_0 \rightarrow \pm V_1$), with V_1 up to 0.2 V that are almost identical and independent of the polarity of V_1.

6. Conclusions

This study provides a better understanding about the nature, motion, generation and recombination of charges in nonpolar liquids. Apparently, in the model system of OLOA 11K in dodecane, different variants of charged inverse micelles (CIMs) exist, each with its own properties. The regular CIMs form a double layer at the electrodes while the generated CIMs end up in the interface layer. Most of them release their charge at the electrode and become neutral micelles, but negatively charged SCIMs retain their charge and can be released when the field changes sign. We hypothesize that the origin of these differences lies in the location of the electric charge inside the CIM: for regular CIMs the charge is in the middle and remains stable; for SCIMs the charge is closer to the interface of the micelle and relatively stable; for most of the generated CIMs the charge is on the surface of the micelle and is released upon contact with the electrode. Transient current measurements are a good tool to study the nature, the electrodynamics, the generation and reduction of different types of charges. It is found that a numerical model based on drift and diffusion of regular CIMs, in combination with the space-charge-limited release of special charged inverse micelles can explain most of the experiments.

View Article Online
DOI: 10.1039/C6CP03544B

Acknowledgments

This research was supported by the Research Foundation-Flanders (FWO-Vlaanderen), IWT, the IAP project photonics@be funded by the Belgian Science Policy program, and the Hercules Foundation.

References

(1) Morrison, I. D. Electrical Charges in Nonaqueous Media. *Colloids Surfaces a-Physicochemical Eng. Asp.* **1993**, *71* (1), 1–37.

(2) Hsu, M. F.; Dufresne, E. R.; Weitz, D. a. Charge Stabilization in Nonpolar Solvents. *Langmuir* **2005**, *21* (5), 4881–4887.

(3) Roberts, G. S.; Sanchez, R.; Kemp, R.; Wood, T.; Bartlett, P. Electrostatic Charging of Nonpolar Colloids by Reverse Micelles. *Langmuir* **2008**, *24* (17), 6530–6541.

(4) Eicke, H. F.; Borkovec, M.; Das-Gupta, B. Conductivity of Water-in-Oil Microemulsions: A Quantitative Charge Fluctuation Model. *J. Phys. Chem.* **1989**, *93* (1), 314–317.

(5) Beunis, F.; Strubbe, F.; Karvar, M.; Drobchak, O.; Brans, T.; Neyts, K. Inverse Micelles as Charge Carriers in Nonpolar Liquids: Characterization with Current Measurements. *Current Opinion in Colloid and Interface Science*. 2013, pp 129–136.

(6) Dukhin, A. S.; Goetz, P. J. How Non-Ionic "electrically Neutral" Surfactants Enhance Electrical Conductivity and Ion Stability in Non-Polar Liquids. *J. Electroanal. Chem.* **2006**, *588* (1), 44–50.

(7) Hao, T. Exploring the Charging Mechanisms in Non-Aqueous Multiphase Surfactant Solutions, Emulsions and Colloidal Systems via Conductivity Behaviors Predicted with Eyring's Rate Process Theory. *Phys. Chem. Chem. Phys.* **2016**, *18* (1), 476–491.

(8) Sainis, S. K.; Merrill, J. W.; Dufresne, E. R. Electrostatic Interactions of Colloidal Particles at Vanishing Ionic Strength Electrostatic Interactions of Colloidal Particles at Vanishing Ionic Strength. *Langmuir* **2008**, *24* (November), 13334–13337.

(9) Smith, G. N.; Eastoe, J. Controlling Colloid Charge in Nonpolar Liquids with Surfactants. *Phys. Chem. Chem. Phys.* **2012**, 424–439.

(10) Strubbe, F.; Verschueren, A. R. M.; Schlangen, L. J. M.; Beunis, F.; Neyts, K. Generation Current of Charged Micelles in Nonaqueous Liquids: Measurements and Simulations. *J. Colloid Interface Sci.* **2006**, *300*, 396–403.

(11) Verschueren, A. R. M.; Notten, P. H. L.; Schlangen, L. J. M.; Strubbe, F.; Beunis, F.; Neyts, K. Screening and Separation of Charges in Microscale Devices: Complete Planar Solution of the Poisson - Boltzmann Equation. *J. Phys. Chem. B* **2008**, *112*, 13038–13050.

View Article Online
DOI: 10.1039/C6CP03544B

(12) Spinelli, H. J. Polymeric Dispersants in Ink Jet Technology. *Adv. Mater.* **1998**, *10* (15), 1215–1218.

(13) Chen, Y.; Au, J.; Kazlas, P.; Ritenour, a; Gates, H.; McCreary, M. Electronic Paper: Flexible Active-Matrix Electronic Ink Display. *Nature* **2003**, *423* (6936), 136.

(14) Mürau, P.; Singer, B. The Understanding and Elimination of Some Suspension Instabilities in an Electrophoretic Display. *J. Appl. Phys.* **1978**, *49* (1978), 4820–4829.

(15) Comiskey, B.; Albert, J. D.; Yoshizawa, H.; Jacobson, J. An Electrophoretic Ink for All-Printed Reflective Electronic Displays. *Nature* **1998**, *394* (July), 253–255.

(16) Bartlett, P.; Campbell, A. I. Three-Dimensional Binary Superlattices of Oppositely Charged Colloids. *Phys. Rev. Lett.* **2005**, *95* (12), 1–4.

(17) Tettey, K. E.; Yee, M. Q.; Lee, D. Layer-by-Layer Assembly of Charged Particles in Nonpolar Media. *Langmuir* **2010**, *26* (12), 9974–9980.

(18) Leunissen, M. E.; Christova, C. G.; Hynninen, A.-P.; Royall, C. P.; Campbell, A. I.; Imhof, A.; Dijkstra, M.; van Roij, R.; van Blaaderen, A. Ionic Colloidal Crystals of Oppositely Charged Particles. *Nature* **2005**, *437* (7056), 235–240.

(19) Hao, T. Electrorheological Fluids. *Adv. Mater.* **2001**, *13* (24), 1847–1857.

(20) Beunis, F.; Strubbe, F.; Marescaux, M.; Beeckman, J.; Neyts, K.; Verschueren, A. R. M. Dynamics of Charge Transport in Planar Devices. *Phys. Rev. E. Stat. Nonlin. Soft Matter Phys.* **2008**, *78* (1 Pt 1), 011502.

(21) Kornilovitch, P.; Jeon, Y. Transient Electrophoretic Current in a Nonpolar Solvent. *J. Appl. Phys.* **2011**, *109* (May).

(22) Parent, M. E.; Yang, J.; Jeon, Y.; Toney, M. F.; Zhou, Z.-L.; Henze, D. Influence of Surfactant Structure on Reverse Micelle Size and Charge for Nonpolar Electrophoretic Inks. *Langmuir* **2011**, *27* (19), 11845–11851.

(23) Prasad, M.; Beunis, F.; Neyts, K.; Strubbe, F. Switching of Charged Inverse Micelles in Non-Polar Liquids. *J. Colloid Interface Sci.* **2015**, *458*, 39–44.

(24) Karvar, M.; Strubbe, F.; Beunis, F.; Kemp, R.; Smith, A.; Goulding, M.; Neyts, K. Transport of Charged Aerosol OT Inverse Micelles in Nonpolar Liquids. *Langmuir* **2011**, *27*, 10386–10391.

(25) Strubbe, F.; Prasad, M.; Beunis, F. Characterizing Generated Charged Inverse Micelles with Transient Current Measurements. *J. Phys. Chem. B* **2015**, *119* (5), 1957–1965.

(26) Karvar, M.; Strubbe, F.; Beunis, F.; Kemp, R.; Smith, N.; Goulding, M.; Neyts, K. Investigation of Various Types of Inverse Micelles in Nonpolar Liquids Using Transient Current Measurements. *Langmuir* **2014**, *30* (41), 12138–12143.

(27) Guo, Q.; Singh, V.; Behrens, S. H. Electric Charging in Nonpolar Liquids because of Nonionizable Surfactants. *Langmuir* **2010**, *26* (22), 3203–3207.

View Article Online
DOI: 10.1039/C6CP03544B

(28) Prieve, D. C.; Hoggard, J. D.; Fu, R.; Sides, P. J.; Bethea, R. Two Independent Measurements of Debye Lengths in Doped Nonpolar Liquids. *Langmuir* **2008**, *24* (4), 1120–1132.

(29) Prasad, M.; Strubbe, F.; Beunis, F.; Neyts, K. Different Types of Charged-Inverse Micelles in Nonpolar Media. *Langmuir* **2016**, *32* (23), 5796–5801.

(30) Rose, A. Space-Charge-Limited Currents in Solids. *Phys. Rev.* **1955**, *97* (6), 1538–1544.

(31) Dielectrics, O. S.; Chan, H.-K. A General Conductivity Expression for Space-Charge-Limited Conduction in Ferroelectrics and Other Solid Dielectrics. *Ferroelectr. Model.* **2005**, No. i.

(32) Orden, D.; Santos, F. Geometry 2003. *Most* **2003**, *528*, 509–528.